

Technical Note

TECHNICAL NOTES are short manuscripts describing new developments or important results of a preliminary nature. These Notes cannot exceed 6 manuscript pages and 3 figures; a page of text may be substituted for a figure and vice versa. After informal review by the editors, they may be published within a few months of the date of receipt. Style requirements are the same as for regular contributions (see inside back cover).

Use of Multiple Actuators for Jet Vectoring

LaTunia Pack-Melton*

NASA Langley Research Center, Hampton, Virginia

and

Avi Seifert†

Tel-Aviv University, 69978 Tel-Aviv, Israel

Introduction

MODIFICATION of the evolution and characteristics of turbulent jets is of great practical importance. Such modification can lead to noise attenuation, mixing and spreading enhancement or reduction, and thrust vectoring. The relevance of coherent structures to the evolution and control of turbulent jets is widely accepted,¹ as is the relationship to stability theory,^{2,3} even though the background flow is turbulent and the amplitudes are finite. It was envisioned² and later demonstrated^{4,5} that nonlinear interaction between different unsteady modes could lead to a mean flow distortion in the form of enhanced mixing or vectoring. However, the expected modification is dependent on the magnitude of the coupling between the linear modes that tend to saturate. It was demonstrated experimentally^{6,7} and numerically⁸ that the presence of a confinement at the jet exit promotes the generation of coherent structures. These in turn interact with the jet flow and with the wall to locally reduce the static pressure and pull the jet flow toward the wall. High-amplitude periodic excitation can also push the jet away from the excited shear layer.^{6,7} When introduced into opposite shear layers, each mode could deflect the jet flow in the same direction. The next logical step would be to combine the two modes to increase the overall effect. In doing so, additional parameters come into play such as the relative frequency and amplitude as well as the phase lag between the two actuators.

The effects of combining the two modes while operating at the same frequency and varying the relative phase are under current investigation. In most cases, the amplitudes were tuned such that each actuator generated a similar jet modification when operated alone.

Experiment Setup

Figures 1a and 1b show schematics of the jet front and top views, respectively. The jet exit diameter D was 39 mm. A 1-mm-wide slot, divided into four equal segments, surrounded the jet exit as shown in

Fig. 1a. Each segment of the slot was connected to a cavity, allowing independent excitation of every 90 deg of the jet circumference. Streamwise excitation (X -excitation) was introduced through the 90-deg segment of the slot surrounding the right-hand side of the jet (positive z , see Fig. 1a). Cross-stream excitation (R -excitation) was introduced through the 90-deg segment of the slot surrounding the left-hand side of the jet (negative z , Fig. 1a). Trip grit (#36) was placed upstream of the jet exit to ensure that the flow at the jet exit was turbulent. All of the data presented in this paper are for a jet exit velocity of $U_e = 12$ m/s, resulting in $Re_D = 31,000$.

A short, wide-angle diffuser was attached at the jet exit. The diffuser half-angle φ was 30 deg and its length L was $1.85 D$. The diffuser could have been significantly shorter and yet still effective.⁷ The inlet geometry of the diffuser was different on each side of the jet exit to allow periodic excitation to be introduced in the streamwise (X) direction on one side of the jet and in the cross-stream (R) direction on the other side (Fig. 1b).

Two zero-mass-flux piezoelectric actuators, each with a resonant frequency of approximately $f \approx 700$ Hz, were used to generate the periodic excitation. The actuators were calibrated as described in Ref. 9. The maximum rms of the velocity fluctuations, u'_{\max} , when operated at 700 Hz using X -excitation, was about 18 m/s. The value of u'_{\max} was about 10% lower for the R -excitation.

The hot-wire data were acquired using a 16-bit analog-to-digital converter. The sampling rate was 12.8 kHz, and the input was low-pass filtered at 5 kHz. The actuators were driven sinusoidally using

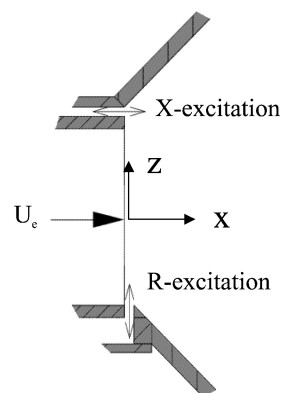
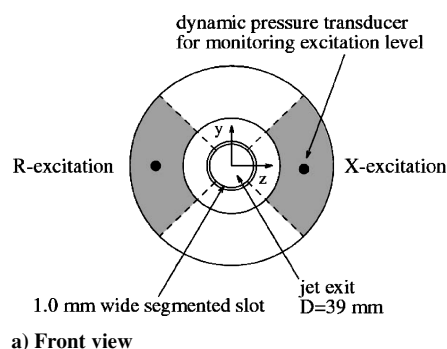


Fig. 1 Schematic of the jet facility: a) front view and b) enlarged view of the jet diffuser and actuators details (top view).

Received 27 January 2003; revision received 12 December 2003; accepted for publication 12 December 2003. Copyright © 2004 by LaTunia Pack-Melton and Avi Seifert. Published by the American Institute of Aeronautics and Astronautics, Inc., with permission. Copies of this paper may be made for personal or internal use, on condition that the copier pay the \$10.00 per-copy fee to the Copyright Clearance Center, Inc., 222 Rosewood Drive, Danvers, MA 01923; include the code 0748-4658/04 \$10.00 in correspondence with the CCC.

*Research Engineer, Flow Physics and Control Branch; l.p.melton@larc.nasa.gov. Member AIAA.

†Senior Lecturer, Department of Fluid Mechanics and Heat Transfer, School of Mechanical Engineering, Faculty of Engineering; also Visiting Scientist, National Institute of Aerospace, Hampton, VA; Seifert@eng.tau.ac.il. Associate Fellow AIAA.

a two-channel variable-phase function generator combined with a multichannel power amplifier. The phase resolution of the function generator was 1 deg.

The velocities measured with the hot-wire are accurate to within $\pm 2\%$. The hot-wire position (x , y , or z) is accurate to within ± 0.04 mm, Re_D is accurate to within $\pm 3\%$, and $\langle c_\mu \rangle$ (defined as $(A_s u_s^2)/(A_j U_e^2)$, where A_s and A_j are the cross-sectional areas of the active slot and of the jet exit respectively, and u_s is the rms of the slot excitation velocity) is accurate to within $\pm 15\%$. The jet deflection estimates (δ) are not different by more than ± 1.5 deg, regardless of the determination method (profile (δ_{pr}) vs plane (δ_{pl})).⁹ However, when calculated from a single hot-wire profile measured at the jet centerplane and considering the excitation effect on the central part of the jet, δ_{pl} is ± 0.25 deg accurate, as inferred from the agreement between the hot wire and the five-hole-probe data.⁹

Discussion of Results

Overview of Jet Excitation Modes

Hot-wire surveys of the jet were acquired at a cross-stream plane of $x/D = 2.5$ and $Re_D = 3.1 \times 10^4$. Streamwise and cross-stream excitation levels were chosen to produce a jet deflection between 2.5 and 3.0 deg using either excitation. Figure 2 shows the contours of the mean velocities for the various excitation types used. The baseline ($\langle c_\mu \rangle_X = \langle c_\mu \rangle_R = 0$) flowfield velocity contours superimposed on Figs. 2a–2d are circular as expected. Slight deviations from a circular pattern are believed to be due to the presence of different slot configurations affecting the jet boundary conditions. Cross-stream excitation with $F^+ = 4.2$ (where $F^+ \equiv fL/U_e$, L is the length of the diffuser, and $F_D^+ \equiv fD/U_e = F^+/1.85$) and $\langle c_\mu \rangle_R = 1.5\%$, which was applied on the left-hand side of the jet, deflected the jet by $\delta_{pl} \approx 3.0$ deg toward the right-hand side, as shown in Fig. 2a, causing the jet also to contract in the z direction and expand in the y direction with respect to the baseline. Streamwise excitation with $F^+ = 4.2$ and $\langle c_\mu \rangle_X = 0.58\%$ deflected the jet by $\delta_{pl} \approx 2.6$ deg toward the excited shear layer (right-hand side) and increased the jet spreading on the excited shear-layer side (Fig. 2b).

In this Note, the effect of combining the cross-stream and streamwise excitations that were applied on opposing sides of the jet is examined. The streamwise and cross-stream excitations are combined in-phase ($\phi = 0$ deg) in Fig. 2c. The velocity contours in Fig. 2c indicate that the overall effect is similar to that seen when exciting the flow using the R -excitation alone (Fig. 2a). However, the streamwise velocity (U) contours for the $\phi = 0$ deg excitation are slightly more spread in the z direction and less spread in the y direction than the R -excitation U contours (Fig. 2a). The jet deflection resulting from the in-phase combination of the two excitations is $\delta_{pl} \approx 6$ deg, about the same as the sum of the individual effects. This type of excitation allows the jet to be deflected efficiently with only moderate spreading. The out-of-phase ($\phi = 180$ deg) combination of R - and X -excitations results in a jet deflection of $\delta_{pl} \approx 7$ deg, approximately the sum of the deflections obtained when exciting the jet with each excitation separately. The velocity contours of Fig. 2d indicate that the effect of the $\phi = 180$ deg excitation is similar to that of the $\phi = 0$ deg excitation on the left-hand side of the jet. The effect of streamwise excitation is more evident in the $\phi = 180$ deg contours on the right-hand side, similar to the effect of the X -excitation alone (Fig. 2b). The observed effect of the relative phase between the two actuators, even at high Strouhal numbers that far exceed the range of unstable frequencies of the jet column, indicates that further study is required to optimize jet flow control using multiple actuators.

Optimal Deflection Angle

The maximum deflection angles in the current setup using either R or X -excitation with $\langle c_\mu \rangle \approx 5\%$, are 8.5 and 9 deg, respectively, as shown in Fig. 3. To generate larger deflection angles, the two modes of excitation were combined. The deflection angles produced by the optimal combination of the two excitations are also presented in Fig. 3. The $\langle c_\mu \rangle_{(X+R)}$ values are a sum of the $\langle c_\mu \rangle$ values generated by each actuator. Much higher deflection angles can be obtained when the two modes of excitation are operated simultaneously with the appropriate phase shift. For instance, using $\langle c_\mu \rangle_{(X+R)} \approx 5\%$, a

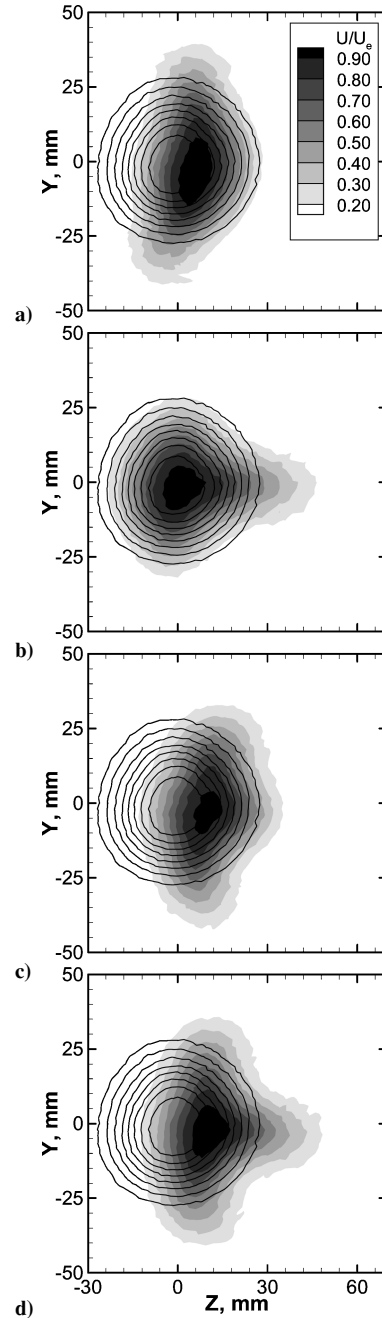


Fig. 2 Baseline (lines) and controlled (grayscale) streamwise velocity contours measured at $x = 2.5 D$: a) R -excited jet, $F^+ = 4.2$ and $\langle c_\mu \rangle_R = 1.5\%$, b) X -excited jet, $F^+ = 4.2$ and $\langle c_\mu \rangle_X = 0.58\%$, c) $X + R$, $\phi = 0$ deg excited jet, d) $X + R$, $\phi = 180$ deg excited jet; in c and d, $F^+ = 4.2$ and $\langle c_\mu \rangle_{X+R} = 2.08\%$.

deflection angle of 13 deg is obtained, based on the curve fit in Fig. 3. This is an increase of about 50% with respect to the effect of any single actuator at the same $\langle c_\mu \rangle$. A maximum deflection of about 15 deg is obtained for $\langle c_\mu \rangle_{(X+R)} \approx 8\%$. The details of the optimal phase will be discussed later. Jet deflection angles that were generated by optimally phased ($X + R$) excitation were compared with jet deflection angles computed by adding the deflection angles from the individual X and R -excitations. It was found⁹ that optimally phased excitation produces jet deflection angles that are similar to and slightly higher than the sum of the individual jet deflection angles produced by the X and R -excitations over the entire $\langle c_\mu \rangle$ range. This result should not be considered trivial because, with a nonoptimal phase shift between the two actuators, the resulting deflection could be significantly smaller than the sum of the deflections due to any single actuator, as will be shown in what follows.

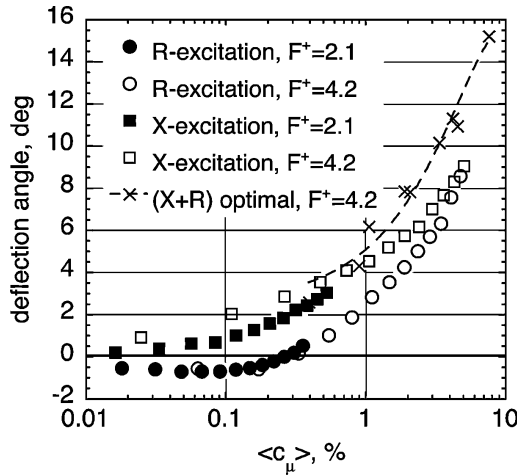


Fig. 3 Jet deflection angles calculated from data measured at $x/D = 2.5$, $ReD = 3.1 \times 10^4$. Excitation mode and frequency indicated in legend.

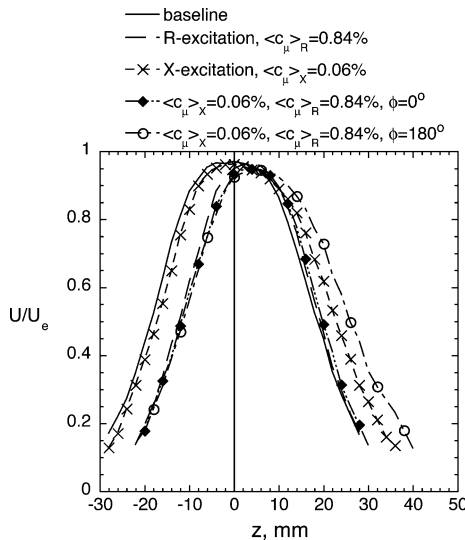


Fig. 4 Hot-wire mean velocity profiles measured at $x/D = 2.5$, $ReD = 3.1 \times 10^4$; $F^+ = 4.2$; excitation mode, momentum coefficient, and phase indicated in legend.

Baseline and controlled-jet U velocity profiles using $F^+ = 4.2$, $\langle c_\mu \rangle_X = 0.06\%$, and $\langle c_\mu \rangle_R = 0.84\%$ are presented in Fig. 4. X -Excitation primarily affects the right-hand side (positive z) of the jet producing a jet deflection of 1.5 deg. R -Excitation mainly affects the left-hand side (negative z) of the jet, producing a jet deflection of 2.0 deg. In-phase, $\phi = 0$ deg, dual-mode excitation appears to diminish the effect of the X -excitation, producing a jet deflection of only 2.4 deg. The $\phi = 180$ deg dual-mode excitation produces a jet deflection of 4.3 deg. This deflection is larger than the sum of the deflection angles $\delta_{pr,X} \approx 1.5$ and $\delta_{pr,R} \approx 2.0$ deg, produced by the X and R -excitations alone.

The sensitivity of the jet deflection angle to the relative phase between the X and R -excitations is presented in Fig. 5 for relatively low values of $\langle c_\mu \rangle$. The jet deflection angles have all been referenced to the sum of the individual deflection angles, $\delta_X + \delta_R$. It is clearly demonstrated that $\phi = 0$ deg is not the optimal combination. The in-phase ($\phi = 0$ deg) combination of the two excitations leads to a reduction in the effectiveness of the combined excitation compared to a linear superposition of the individual effects. The jet deflection angles obtained for the $\langle c_\mu \rangle$ levels presented in Fig. 5 indicate that the optimum phase angle is $\phi = \pi \pm \pi/6$. A comparison of the $\langle c_\mu \rangle$ levels presented for the $F^+ = 4.2$ cases indicates that the ϕ sensitivity decreases with increasing $\langle c_\mu \rangle$. A comparison of the two frequencies

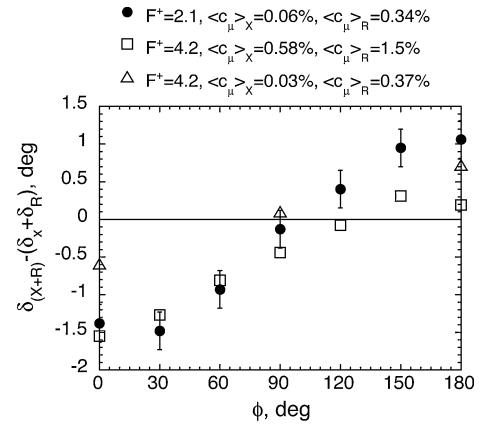


Fig. 5 Dependence of jet deflection angles on phase angle between X - and R -excitation modes; δ_{pr} presented. Note that δ uncertainty is $\pm 0.25^\circ$ for the entire data set.

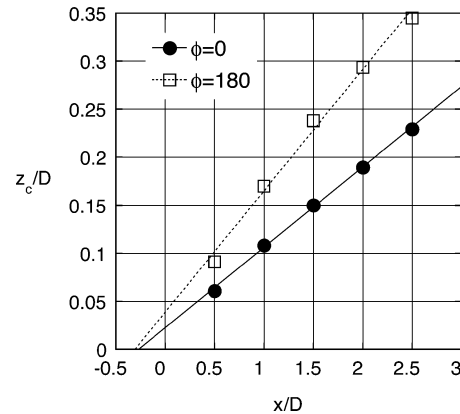


Fig. 6 Streamwise variation of jet center of linear streamwise momentum: $F^+ = 4.2$, $\langle c_\mu \rangle_X = 0.14\%$, and $\langle c_\mu \rangle_R = 1.76\%$.

presented in Fig. 5 indicates that the ϕ sensitivity at $F^+ = 2.1$ is greater than that at $F^+ = 4.2$ for the $\langle c_\mu \rangle$ range examined.

Velocity profiles measured at $x/D = 2.5$ and $y/D = 0.0$ for varying phase using $(X + R)$ excitation with $F^+ = 4.2$, $\langle c_\mu \rangle_X = 0.6\%$, and $\langle c_\mu \rangle_R = 1.6\%$ (not shown, Ref. 9) indicate that the effect of increasing phase is mainly to enhance the jet spreading on the X -excited side of the jet. Profiles of u' (not shown) indicate that the velocity fluctuations increase on the R -excitation side with increasing phase, whereas they decrease on the X -excitation side, as a result of the enhanced spreading and reduced shear. From this point we shall concentrate on $\phi = 0$ and $\phi = 180$ deg, while noting that an optimal performance at low $\langle c_\mu \rangle$ could be found at $\phi = \pi \pm \pi/6$.

The results presented thus far have focused on the effect of the R and X -excitations at a single streamwise location, $x/D = 2.5$. In this section, data closer to the excitation source and the jet exit were examined to determine if the global effects measured at $x/D = 2.5$ represent flow behavior near the source and to learn more about the physical mechanism causing the observed results. The change in the center of momentum, z_c , with axial location is shown in Fig. 6 for the in-phase and 180-deg out-of-phase combination of the X and R -excitations using $F^+ = 4.2$, $\langle c_\mu \rangle_X = 0.14\%$, and $\langle c_\mu \rangle_R = 1.76\%$. The jet deflection angles produced by the R and X -excitations independently are $\delta_{pr,R} = 4.4$ and $\delta_{pr,X} = 3.2$ deg. The $\phi = 0$ deg combination of the X and R -excitations results in a deflection angle of 5.1 deg, and the $\phi = 180$ deg combination of the two excitations results in a deflection angle of 7.7 deg. These deflection angles were computed based on data measured at $x/D = 2.5$. Deflection angles computed from data taken closer to the source are smaller due to the fact that the virtual origin of the deflected jet is close to $x/D = -0.25$ (Fig. 6). The jet deflection angle can also be computed from the inverse tangent of the slopes of the curves in Fig. 6. This

approach yields jet deflection angles of 4.9 and 7.2 deg for $\phi = 0$ and $\phi = 180$ deg, respectively. These results are in good agreement with the jet deflection angles based on the shift in linear momentum measured at $x/D = 2.5$ (5.1 and 7.7 deg, respectively).

Summary

Two actuators placed on opposite sides of a circular jet with a short, wide-angle diffuser attached at the jet exit were activated simultaneously to control the jet vectoring and spreading. One actuator slot covered a $\pi/2$ segment at the right-hand side shear layer and was pointed in the streamwise direction. A second actuator slot, which also covered a $\pi/2$ segment, was placed in the opposite shear layer and generated cross-stream excitation. When operated alone, each actuator was capable of vectoring the jet to the right-hand side. The effectiveness of the streamwise excitation was greater than that of the cross-stream excitation. However, the two actuators were operated together at the same frequency in an attempt to increase the obtainable deflection angles. It was demonstrated that with proper phase tuning of the two zero-mass-flux actuators, it is possible to obtain deflection angles equal to or greater than the sum of the effects of each actuator when operating individually, whereas a nonoptimal phase lag caused a significant reduction in the resulting vectoring angle compared to the sum of the two effects. At low to medium periodic momentum input levels, a phase shift of $\pi \pm \pi/6$ was found to provide an optimum response. The practical aspect of these findings is that it would be possible to combine several actuators of modest control authority and generate a strong global effect that could be at least equal to the linear combination of the individual effects.

Acknowledgments

The authors would like to thank NASA Langley Flow Physics and Control Branch members Steve Wilkinson, Ponnampalam Balakumar, George Beeler, Anthony Washburn, Mike Walsh, and William Sellers for their support.

References

- ¹Crow, S. C., and Champagne, F. H., "Orderly Structure in Jet Turbulence," *Journal of Fluid Mechanics*, Vol. 48, No. 3, 1971, pp. 547–591.
- ²Michalke, A., "Survey on Jet Instability Theory," *Progress in Aerospace Sciences*, Vol. 21, No. 3, 1984, pp. 159–199.
- ³Gaster, M., Kit, E., and Wygnanski, I., "Large-Scale Structures in a Forced Turbulent Mixing Layer," *Journal of Fluid Mechanics*, Vol. 150, 1985, pp. 23–39.
- ⁴Cohen, J., and Wygnanski, I., "The Evolution of Instabilities in the Axisymmetric Jet. Part 1. The Linear Growth of Disturbances near the Nozzle," *Journal of Fluid Mechanics*, Vol. 176, 1987, pp. 191–219.
- ⁵Wygnanski, I., and Peterson, R. A., "Coherent Motion in Excited Free Shear Flows," AIAA Paper 85-0539, March 1985.
- ⁶Alvi, F. S., Strykowski, P. J., Krothapalli, A., and Forliti, D. J., "Vectoring Thrust in Multiaxes Using Confined Shear Layers," *Journal of Fluid Engineering*, Vol. 122, No. 1, March 2000, pp. 3–13.
- ⁷Pack, L. G., and Seifert, A., "Periodic Excitation for Jet Vectoring and Enhanced Spreading," *Journal of Aircraft*, Vol. 38, No. 3, 2001, pp. 486–495.
- ⁸Grinstein, F. F., and DeVore, C. R., "Entrainment and Thrust Vector Control with Countercurrent Rectangular Jets," AIAA Paper 99-00165, Jan. 1999.
- ⁹Pack, L. G., and Seifert, A., "Multiple Mode Actuation of a Turbulent Jet," AIAA Paper 01-0735, Jan. 2001.

Physics of Direct Hit and Near Miss Warhead Technology

Richard M. Lloyd, Raytheon Electronic Systems

This book presents a new class of warheads utilizing "near miss and direct hit warhead technology." These warheads use nearly all of their total volume and mass as damage mechanisms, deploying 10–30 times more mass when compared with today's warheads.

Currently, most missiles and kill vehicles are direct hit only and do not contain a warhead mechanism. This book provides warhead designers with a better understanding of the kill requirements and vulnerabilities of ballistic missile payloads to design an optimum direct hit missile or warhead. It also describes the challenges of designing small, lethality enhancement technologies that can be implemented by direct hit kill vehicles, as well as an anti-ballistic missile warhead with varying tactical ballistic missile payloads, including chemical submunitions, unitary high explosives, and nuclear payloads.

Contents:

Introduction to Physics of Warheads Against Ballistic Missiles • Fragmentation Warhead Principles • Premade Fragment Warheads • KE-Rod Warheads • Direct Energy Warheads • Blast Warhead Concepts • Direct Hit Modeling with Missile Debris Considerations • Terminal Encounter Kinematics • Target Detection Mechanics Coupled with Designing Warheads • Vulnerability Modeling • Warhead Design with Endgame Codes • Warhead Evaluation Principles

Features more than 300 four-color illustrations.

Progress in Astronautics and Aeronautics
Sep 2001, 636 pp, Hardcover
ISBN 1-56347-473-5
List Price: \$100.95
AIAA Member Price: \$69.95
Source: 945



American Institute of Aeronautics and Astronautics

Publications Customer Service, P.O. Box 960, Herndon, VA 20172-0960
Fax: 703/661-1501 • Phone: 800/682-2422 • E-mail: warehouse@aiaa.org
Order 24 hours a day at www.aiaa.org